Journal of Structural Chemistry. Vol. 47, No. 5, pp. 894-905, 2006
Original Russian Text Copyright © 2006 by T. M. Polyanskaya, V. A. Nadolinnyi, V. V. Volkov, E. A. Il'inchik, and M. K. Drozdova

SYNTHESIS, X-RAY STRUCTURAL AND SPECTROSCOPIC STUDY OF [*bis*(1,10-PHENANTHROLINIUM)](1+) {3,3′-*commo-bis*-[η^5-1,2-DICARBA-(3)-NICKEL(III)-*closo*-DODECABORATE]}(1-), $[H(1,10\text{-}C_{12}H_8N_2)_2]^+\{Ni^{III}[\eta^5\text{-}(3)\text{-}1,2\text{-}B_9C_2H_{11}]_2\}^-$

T. M. Polyanskaya, V. A. Nadolinnyi, V. V. Volkov,
E. A. Il'inchik, and M. K. Drozdova

UDC 548.736:546.74:271:543:422:541.139

A new compound comprising a Ni(III) di-carbollide cluster anion $[H(Phen)_2][Ni(B_9C_2H_{11})_2]$, Phen = 1,10-phenanthroline, has been prepared and structurally characterized. Crystal data: $C_{28}H_{39}B_{18}N_6Ni$, $M = 684.92$, monoclinic, space group $P2_1/n$; unit cell parameters: $a = 19.337(3)$ Å, $b = 6.9968(8)$ Å, $c = 25.630(4)$ Å; $\beta = 101.69(1)°$; $V = 3395.8(9)$ Å^3, $Z = 4$, $d_{\text{calc}} = 1.340$ g/cm^3, $T = 293$ K, $F(000) = 1412$, $\mu = 0.602$ mm^{-1}. The structure was solved by the direct and Fourier methods and refined in the full-matrix anisotropic approximation (isotropic for hydrogen atoms) to final agreement factors $R_1 = 0.0372$, $wR_2 = 0.0887$ for 4136 $I_{hkl} \geqslant 2\sigma_I$ from 5445 measured I_{hkl} (an Enraf-Nonius CAD-4 diffractometer, λMoK_α, graphite monochromator, ω-scanning). The structure is built from $[H(Phen)_2]^+$ cations and $[Ni(C_2B_9H_{11})_2]^-$ anions. The anions have a usual for *commo*-metal carboranes sandwich structure consisting of two icosahedra $\{NiC_2B_9\}$ sharing a common Ni vertex. EPR technique shows that nickel ion has the electron state $3d^7$ with $S = 1/2$. The angular dependence of single-crystal EPR spectra was used to calculate g-factors ($g_1 = 2.0803$, $g_2 = 2.0229$ and $g_3 = 1.9810$) and to assign principal values of the **g**-tensor to the directions in the crystal structure, in accord with which g_1 is directed along the Cb–Ni–Cb axis, while the direction and the value of g_2 is determined by a distortion introduced by the cation. The compound has been characterized by IR and Raman spectroscopy.

Keywords: crystal structure, cluster, metal carborane, nickel, 1,10-phenanthroline, EPR spectra, vibrational spectra.

INTRODUCTION

This work is a continuation of the studies on complicated systems of salt-like complexes including the derivatives of planar aromatic heterocycles and cluster derivatives of *ortho*-carborane(12), the latter being tri-dimensional aromatic systems [1-7]. The particular subject of investigation is the title complex $[H(1,10\text{-}C_{12}H_8N_2)_2]^+\{Ni^{III}[\eta^5\text{-}\pi\text{-}(3)\text{-}1,2\text{-}B_9C_2H_{11}]_2\}^-$. Let us denote the cation as $[H(Phen)_2]^+$. $\{Ni^{III}[\eta^5\text{-}\pi\text{-}(3)\text{-}1,2\text{-}B_9C_2H_{11}]_2\}^-$ was named in the work [8]. Hereafter, the anionic ligand $[1,2\text{-}(3)\text{-}B_9C_2H_{11}]^{2-}$ is termed Cb^{2-}, and the whole anion — $NiCb_2^-$. Ni(III) ion within the anion has the electronic configura-

---

A. V. Nikolaev Institute of Inorganic Chemistry, Siberian Division, Russian Academy of Sciences, Novosibirsk; polyan@che.nsk.su. Translated from *Zhurnal Strukturnoi Khimii*, Vol. 47, No. 5, pp. 905-916, September-October, 2006. Original article submitted March 7, 2005.

tion $3d^7$ with one unpaired electron. Therefore, $NiCb_2^-$ is paramagnetic and can be explored by magnetochemistry and EPR methods [1, 9, 10]. Experimental values of 1.76-1.81 BM (Bohr magnetons) weakly depending on the cation environment have been reported for the effective magnetic moment μ_{ef} of $NiCb_2^-$ [1]; a spin-only value of the magnetic moment is 1.73 BM.

We have prepared this complex, $[H(Phen)_2]^+(NiCb_2)^-$ **1,** in the attempt to synthesize a simpler salt $(HPhen)^+(NiCb_2)^-$ by depositing this salt from the aqueous medium (pH 4.56, acetate buffer) treating a solution of the $Cs[NiCb_2]$ salt with $(HPhen)^+$. However, as X-ray structural analysis and elemental analysis reveal, the product obtained has the composition $[H(Phen)_2]^+(NiCb_2)^-$. The products of the synthesis also included $[Ni^{IV}Cb_2]^0$, insoluble in water but soluble in organic solvents.

Compounds of this cation and boron-containing anions have not been studied before. The target of this work is the investigation of this newly prepared complex with X-ray diffraction and spectroscopic methods.

EXPERIMENTAL

Synthesis of $[H(Phen)_2][NiCb_2]$, $C_{28}H_{39}N_4B_{18}Ni$, was performed by the reaction $Cs[Ni(B_9C_2H_{11})_2] + 2Phen + H^+ = [H(Phen)_2][Ni(B_9C_2H_{11})] + Cs^+$. The reaction was carried out in a slightly acidic water medium with pH 4.56 (acetate buffer). A 0.649 g (2.23 mmol) sample of $Phen{\cdot}H_2O$ (purum) was dissolved in 300 ml of the acetate buffer. 0.944 g, (2.00 mmol) of $Cs[NiCb_2]$ was dissolved in 200 ml of hot water with the addition of Na_2SO_3 (a reducing agent to prevent Ni^{3+} oxidation). The solutions were combined under vigorous stirring to yield a yellow flake-like amorphous precipitate. The precipitate formed was filtered off, washed with water and dried in air on the filter, and then washed with warm benzene (to remove the admixture of $[Ni^{IV}Cb_2]^0$ formed). The precipitate was dried *in vacuo* at 60°C until a constant weight was reached. $[H(Phen)_2][NiCb_2]$ thus obtained had the weight of 0.832 g (1.22 mmol) corresponding to 61% yield on $Cs[NiCb_2]$. Additionally, 0.02 g of $[NiCb_2]^0$ was isolated from the washing benzene. The composition of the compound was confirmed by chemical analysis methods. Found, wt %: H^+ 0.145, Phen 51.50, Ni 8.36, B 27.70. For $C_{28}H_{39}N_4B_{18}Ni$ calculated, %: H^+ 0.147, Phen 52.61, Ni 8.57, B 28.43.

Compound **1** is fairly stable when stored in a desiccator, insoluble in water and hydrocarbon solvents, soluble in acetonitrile. Crystallization from acetonitrile by water vapor diffusion at room temperature afforded well-shaped solvent-free brown single crystals of X-ray quality. Single crystals have a density of 1.33±0.01 g/cm^3 as measured by flotation.

The data collection was performed on a four-circle automated diffractometer Enraf-Nonius CAD-4 using the standard method (λMoK_α, graphite monochromator, ω-scanning with varying speed at 293 K). Unit cell parameters were refined using 24 centered reflections. The conversion of I_{hkl} to F_{hkl} was carried out with allowance for Lorentz and polarization factors. The absorption correction was calculated from transmission curves based on azimuthal scans for two reflections. During the data collection, three control reflections measured after every 97 reflections did not manifest any intensity decrease, so no decay correction was applied. The structure was solved by the direct and Fourier methods. The direct method implemented in SIR-97 program [11] was used to find coordinates for the majority of non-hydrogen atoms of the structure. The other atoms were located from differential electron density syntheses. The refinement of coordinates, thermal parameters of non-hydrogen atoms and isotropic extinction coefficient was carried with SHELXL-97 program package [12] using the isotropic and then anisotropic full-matrix refinement by the least-square method. All hydrogen atoms were positioned geometrically and were freely refined in the isotropic approximation. Experimental parameters and crystal data along with the structure solution details and refinement are given in Table 1. Positional and equivalent thermal parameters of the independent non-hydrogen atoms are listed in Table 2, cation bond lengths are reported in Table 3, the anion ones in Table 4; bond angles in the cation in Table 5, in the anion in Table 6. Coordinates and isotropic thermal parameters of hydrogen atoms are available from the authors.

EPR spectra were recorded on a Varian E-109 spectrometer operating at 9.5 GHz at the temperatures 77 K and 300 K. Both single crystals and powders of synthesized compound **1** were the subject of the study. The angular dependence

TABLE 1. Crystal Data, Experimental Details, and Structure Refinement Parameters for **1**

Chemical formula	$C_{28}H_{39}B_{18}N_4Ni$
Molecular weight	684.92
Temperature, K	293(2)
Wavelength, Å	0.71069
Crystal system	Monoclinic
Space group	$P2_1/n$
Unit cell parameters: *a*, *b*, *c*, Å	19.337(3), 6.9968(8), 25.630(4)
β, deg	101.69(1)
Volume, Å^3	3395.8(9)
Z	4
Density (calc), g/cm^3	1.340
Absorption coefficient, mm^{-1}	0.602
F(000)	1412
Crystal size, mm	0.32×0.36×1.12
θ range of data collection, deg	1.21-24.97
hkl range of data collection	$0 \leqslant h \leqslant 22$, $0 \leqslant k \leqslant 8$, $-30 \leqslant l \leqslant 29$
Measured/independent reflections	5445/5291 [*R*(*int*) = 0.0119]
Refinement	Full-matrix on F^2
$N_{hkl}/N_{\text{constrains}}/N_{\text{parameters}}$	5291/0/617
GOOF on F^2	0.967
Final *R* factors [$I > 2\sigma(I)$]	$R1 = 0.0372$, $wR2 = 0.0887$
R factors (all data)	$R1 = 0.0470$, $wR2 = 0.0985$
Extinction coefficient	0.00308(8)
Residual peaks in electron density map, e·Å^{-3}	0.429 and –0.565

TABLE 2. Positional (×10^4) and Equivalent Isotropic Thermal Parameters of the Independent Atoms (Å^2×10^3, $U_{eq} = 1/3(U_{11} + U_{22} + U_{33})$) in the Structure of $[H(Phen)_2][Ni(C_2B_9H_{11})_2]$

Atom	*x*	*y*	*z*	U_{eq}	Atom	*x*	*y*	*z*	U_{eq}
1	2	3	4	5	6	7	8	9	10
N(1)	2888(1)	859(1)	7280(1)	41(1)	B(1)	4639(1)	1104(2)	4115(1)	49(1)
N(2)	1535(1)	1647(1)	6738(1)	48(1)	B(2)	4188(1)	–602(2)	3670(1)	43(1)
C(1)	3529(1)	493(1)	7562(1)	45(1)	B(3)	4223(1)	1793(2)	3465(1)	45(1)
C(2)	4081(1)	141(1)	7309(1)	47(1)	B(4)	4185(1)	3293(2)	4013(1)	62(1)
C(3)	3967(1)	199(1)	6769(1)	45(1)	B(5)	4073(1)	1808(2)	4543(1)	58(1)
C(4)	3296(1)	611(1)	6467(1)	38(1)	B(6)	4085(1)	–602(2)	4335(1)	52(1)
C(5)	3145(1)	742(1)	5899(1)	46(1)	C(9A)	3365(1)	–900(1)	3825(1)	44(1)
C(6)	2495(1)	1170(1)	5629(1)	49(1)	B(9)	3365(1)	–900(1)	3825(1)	44(1)
C(7)	1930(1)	1492(1)	5898(1)	46(1)	C(10A)	3427(1)	539(1)	3312(1)	38(1)
C(8)	1239(1)	1958(2)	5630(1)	59(1)	B(10)	3427(1)	539(1)	3312(1)	38(1)
C(9)	725(1)	2233(2)	5914(1)	65(1)	C(8A)	3435(1)	2856(2)	3523(1)	51(1)
C(10)	897(1)	2048(2)	6466(1)	59(1)	B(8A)	3435(1)	2856(2)	3523(1)	51(1)
C(11)	2046(1)	1381(1)	6455(1)	39(1)	C(7A)	3362(1)	2887(2)	4156(1)	56(1)
C(12)	2745(1)	937(1)	6740(1)	36(1)	B(7A)	3362(1)	2887(2)	4156(1)	56(1)
N(3)	2041(1)	0775(1)	8187(1)	39(1)	B(11)	3268(1)	539(2)	4349(1)	43(1)
N(4)	3389(1)	1673(1)	8734(1)	50(1)	B(21)	463(1)	1477(2)	3187(1)	50(1)
C(13)	1387(1)	336(1)	7939(1)	45(1)	B(22)	932(1)	3181(2)	3630(1)	47(1)

TABLE 2. (Continued)

1	2	3	4	5	6	7	8	9	10
C(14)	830(1)	49(1)	8195(1)	47(1)	B(23)	1004(1)	3179(2)	2960(1)	50(1)
C(15)	953(1)	223(1)	8737(1)	46(1)	B(24)	1005(1)	783(2)	2742(1)	51(1)
C(16)	1631(1)	673(1)	9020(1)	38(1)	B(25)	925(1)	–705(2)	3275(1)	59(1)
C(17)	1785(1)	843(1)	9587(1)	46(1)	B(26)	897(1)	775(2)	3836(1)	55(1)
C(18)	2442(1)	1222(1)	9853(1)	49(1)	C(7B)	1779(1)	1972(1)	2974(1)	39(1)
C(19)	3003(1)	1497(1)	9578(1)	45(1)	C(8B)	1742(1)	–295(2)	3134(1)	50(1)
C(20)	3698(1)	1915(2)	9844(1)	63(1)	B(8B)	1742(1)	–295(2)	3134(1)	50(1)
C(21)	4209(1)	2189(2)	9560(1)	70(1)	B(27)	1697(1)	–407(2)	3793(1)	49(1)
C(22)	4031(1)	2067(2)	9008(1)	63(1)	B(28)	1702(1)	2067(2)	4015(1)	45(1)
C(23)	2877(1)	1387(1)	9017(1)	40(1)	C(29)	1735(1)	3427(1)	3460(1)	47(1)
C(24)	2169(1)	935(1)	8729(1)	37(1)	B(29)	1735(1)	3427(1)	3460(1)	47(1)
Ni(1)	2552(1)	1271(1)	3648(1)	31(1)					

TABLE 3. Selected Bond Lengths *d*, Å in the Cation $[H(Phen)_2]$ in the Structure of $[H(Phen)_2][Ni(C_2B_9H_{11})_2]$

Bond	*d*	Bond	*d*	Bond	*d*
N(1)–C(1)	1.3250(10)	C(7)–C(11)	1.4026(11)	C(15)–C(16)	1.4005(11)
N(1)–C(12)	1.3564(10)	C(7)–C(8)	1.4109(12)	C(15)–H(15)	0.981(8)
N(1)–H(1N)	0.763(8)	C(8)–C(9)	1.3574(15)	C(16)–C(24)	1.4083(12)
N(2)–C(10)	1.3190(11)	C(8)–H(8)	0.893(8)	C(16)–C(17)	1.4275(11)
N(2)–C(11)	1.3512(11)	C(9)–C(10)	1.3935(14)	C(17)–C(18)	1.3413(12)
C(1)–C(2)	1.3790(13)	C(9)–H(9)	1.003(8)	C(17)–H(17)	0.970(7)
C(1)–H(1)	0.909(7)	C(10)–H(10)	0.994(8)	C(18)–C(19)	1.4204(13)
C(2)–C(3)	1.3568(12)	C(11)–C(12)	1.4334(10)	C(18)–H(18)	0.917(7)
C(2)–H(2)	0.948(7)	N(3)–C(13)	1.3312(10)	C(19)–C(20)	1.4087(13)
C(3)–C(4)	1.4007(11)	N(3)–C(24)	1.3659(10)	C(19)–C(23)	1.4110(11)
C(3)–H(3)	0.949(8)	N(4)–C(22)	1.3267(11)	C(20)–C(21)	1.3540(15)
C(4)–C(12)	1.4081(12)	N(4)–C(23)	1.3557(11)	C(20)–H(20)	0.948(8)
C(4)–C(5)	1.4273(11)	C(13)–C(14)	1.3840(13)	C(21)–C(22)	1.3895(14)
C(5)–C(6)	1.3397(11)	C(13)–H(13)	0.935(7)	C(21)–H(21)	0.960(8)
C(5)–H(5)	0.967(8)	C(14)–C(15)	1.3640(13)	C(22)–H(22)	0.950(9)
C(6)–C(7)	1.4232(13)	C(14)–H(14)	0.949(7)	C(23)–C(24)	1.4523(10)
C(6)–H(6)	0.938(7)				

TABLE 4. Selected Bond Lengths *d*, Å in the Anion $[Ni(C_2B_9H_{11})_2]$ in the Structure of $[H(Phen)_2][Ni(C_2B_9H_{11})_2]$

Bond	*d*	Bond	*d*	Bond	*d*
1	2	3	4	5	6
Ni(1)–B(11)	2.0974(9)	Ni(1)–C(7B)	2.0989(8)	Ni(1)–C(10A)	2.1121(9)
Ni(1)–C(8A)	2.1150(10)	Ni(1)–B(27)	2.1198(11)	Ni(1)–B(28)	2.1249(10)
Ni(1)–C(8B)	2.1330(10)	Ni(1)–C(7A)	2.1455(10)	B(1)–B(2)	1.7561(15)
B(1)–B(4)	1.7576(17)	B(1)–B(3)	1.7643(14)	B(1)–B(5)	1.7691(16)
B(1)–B(6)	1.7710(16)	B(1)–H(1B)	1.032(7)	B(2)–C(9A)	1.7302(14)
B(2)–B(6)	1.7562(15)	B(2)–C(10A)	1.7606(12)	B(2)–B(3)	1.7615(16)
B(2)–H(2B)	1.071(9)	B(3)–C(8A)	1.7278(14)	B(3)–C(10A)	1.7452(13)
B(3)–B(4)	1.7673(17)	B(3)–H(3B)	1.028(8)	B(4)–C(7A)	1.7280(16)

TABLE 4. (Continued)

1	2	3	4	5	6
B(4)–C(8A)	1.7421(14)	B(4)–B(5)	1.7587(18)	B(4)–H(4B)	1.115(10)
B(5)–C(7A)	1.7013(14)	B(5)–B(6)	1.7706(18)	B(5)–B(11)	1.7747(15)
B(5)–H(5B)	1.045(7)	B(6)–C(9A)	1.7175(13)	B(6)–B(11)	1.7767(15)
B(6)–H(6B)	1.053(8)	C(9A)–C(10A)	1.6808(13)	C(9A)–B(11)	1.7176(14)
C(9A)–H(9B)	1.046(9)	C(10A)–C(8A)	1.7086(14)	C(10A)–H(10B)	1.077(7)
C(8A)–C(7A)	1.6559(15)	C(8A)–H(8BA)	1.047(10)	C(7A)–B(11)	1.7356(16)
C(7A)–H(7C)	1.006(9)	B(11)–H(11B)	0.992(8)	B(21)–B(23)	1.7593(16)
B(21)–B(25)	1.7603(17)	B(21)–B(24)	1.7640(16)	B(21)–B(22)	1.7651(15)
B(21)–B(26)	1.7742(14)	B(21)–H(21B)	1.036(7)	B(22)–C(29)	1.7045(14)
B(22)–B(23)	1.7502(15)	B(22)–B(26)	1.7700(17)	B(22)–B(28)	1.7900(13)
B(22)–H(22B)	0.998(9)	B(23)–C(29)	1.7145(13)	B(23)–C(7B)	1.7150(13)
B(23)–B(24)	1.7671(17)	B(23)–H(23B)	1.076(7)	B(24)–C(7B)	1.7113(13)
B(24)–C(8B)	1.7395(13)	B(24)–B(25)	1.7477(17)	B(24)–H(24B)	1.091(8)
B(25)–C(8B)	1.7127(15)	B(25)–B(26)	1.7818(17)	B(25)–B(27)	1.7968(14)
B(25)–H(25B)	1.074(10)	B(26)–B(27)	1.7782(15)	B(26)–B(28)	1.7793(14)
B(26)–H(26B)	1.040(9)	C(7B)–C(29)	1.6231(13)	C(7B)–C(8B)	1.6439(14)
C(7B)–H(7CB)	0.981(8)	C(8B)–B(27)	1.7084(15)	C(8B)–H(8BB)	1.020(9)
B(27)–B(28)	1.8213(17)	B(27)–H(27B)	1.086(8)	B(28)–C(29)	1.7226(14)
B(28)–H(28B)	1.068(7)	C(29)–H(29B)	0.990(9)		

TABLE 5. Bond Angles φ, deg in the Cation $[H(Phen)_2]^+$

Angle	φ	Angle	φ	Angle	φ
C(1)–N(1)–C(12)	122.58(7)	C(6)–C(5)–C(4)	121.14(8)	N(2)–C(10)–C(9)	124.10(9)
C(10)–N(2)–C(11)	117.07(7)	C(5)–C(6)–C(7)	121.18(7)	N(2)–C(11)–C(7)	123.65(7)
N(1)–C(1)–C(2)	120.47(7)	C(8)–C(7)–C(11)	116.62(8)	N(2)–C(11)–C(12)	118.17(7)
C(3)–C(2)–C(1)	119.40(7)	C(8)–C(7)–C(6)	123.16(8)	C(7)–C(11)–C(12)	118.17(7)
C(2)–C(3)–C(4)	120.84(8)	C(6)–C(7)–C(11)	120.21(7)	N(1)–C(12)–C(4)	118.85(7)
C(3)–C(4)–C(12)	117.85(7)	C(9)–C(8)–C(7)	119.82(8)	N(1)–C(12)–C(11)	120.44(7)
C(3)–C(4)–C(5)	123.54(8)	C(8)–C(9)–C(10)	118.72(8)	C(4)–C(12)–C(11)	120.70(7)
C(12)–C(4)–C(5)	118.61(7)				
C(13)–N(3)–C(24)	117.52(7)	C(18)–C(17)–C(16)	120.97(8)	N(4)–C(22)–C(21)	124.29(9)
C(22)–N(4)–C(23)	117.05(7)	C(17)–C(18)–C(19)	120.96(7)	N(4)–C(23)–C(19)	122.89(7)
N(3)–C(13)–C(14)	124.26(8)	C(20)–C(19)–C(23)	117.08(8)	N(4)–C(23)–C(24)	118.41(7)
C(15)–C(14)–C(13)	118.50(7)	C(23)–C(19)–C(18)	120.40(7)	C(19)–C(23)–C(24)	118.70(8)
C(14)–C(15)–C(16)	119.95(8)	C(20)–C(19)–C(18)	122.52(8)	N(3)–C(24)–C(16)	121.82(7)
C(15)–C(16)–C(24)	117.94(7)	C(21)–C(20)–C(19)	119.88(8)	N(3)–C(24)–C(23)	119.47(7)
C(24)–C(16)–C(17)	121.81(8)	C(20)–C(21)–C(22)	118.80(9)	C(16)–C(24)–C(23)	118.70(7)
C(15)–C(16)–C(17)	121.81(8)				

of nickel ion EPR spectra in the crystal were measured at 77 K. In the calculation of the *g*-factor, 2,2-diphenylpicrylhydrazyl (DPPH) was used as a reference. Spectra were simulated with Simfonia program.

IR spectra were recorded with a spectrophotometer UR-20 in KBr and Vaseline oil.

Raman spectra of solid samples were obtained using a Triplemate SPEX spectrometer equipped with a microscope and a multi-channel detector. The measurements were performed in the back-scattering configuration with 488 nm line of an Ar laser as the exciting source.

TABLE 6. Bond Angles ω, deg in the Anion $[Ni(B_9C_2H_{11})_2]^-$

Angle	ω	Angle	ω	Angle	ω
B(2)–B(1)–B(3)	60.05(6)	B(6)–C(9A)–B(11)	62.29(6)	C(7B)–B(24)–C(8B)	56.89(5)
B(3)–B(1)–B(4)	60.24(6)	B(2)–C(9A)–C(10A)	62.13(6)	C(8B)–B(24)–B(25)	58.83(6)
B(4)–B(1)–B(5)	59.82(7)	B(2)–C(9A)–B(6)	61.25(6)	B(21)–B(24)–B(25)	60.17(7)
B(2)–B(1)–B(6)	59.72(6)	B(3)–C(10A)–C(8A)	60.02(6)	C(7B)–B(24)–B(23)	59.06(6)
B(5)–B(1)–B(6)	60.02(7)	B(2)–C(10A)–C(9A)	60.31(5)	B(21)–B(24)–B(23)	59.76(7)
B(6)–B(2)–C(9A)	59.02(6)	B(2)–C(10A)–B(3)	60.32(6)	C(8B)–B(25)–B(24)	60.34(6)
B(1)–B(2)–B(6)	60.56(6)	B(3)–C(8A)–C(10A)	61.04(6)	B(21)–B(25)–B(24)	60.38(7)
C(9A)–B(2)–C(10A)	57.56(5)	B(4)–C(8A)–C(7A)	61.07(6)	B(21)–B(25)–B(26)	60.11(6)
B(1)–B(2)–B(3)	60.21(6)	B(3)–C(8A)–B(4)	61.24(6)	C(8B)–B(25)–B(27)	58.20(6)
B(3)–B(2)–C(10A)	59.41(5)	B(4)–C(7A)–C(8A)	61.93(6)	B(26)–B(25)–B(27)	59.59(6)
C(8A)–B(3)–C(10A)	58.94(6)	B(4)–C(7A)–B(5)	61.70(7)	B(21)–B(26)–B(22)	59.74(6)
B(2)–B(3)–C(10A)	60.27(5)	B(5)–C(7A)–B(11)	62.17(6)	B(22)–B(26)–B(28)	60.57(6)
B(1)–B(3)–B(2)	59.75(6)	B(5)–B(11)–C(7A)	57.97(6)	B(27)–B(26)–B(28)	61.59(6)
B(4)–B(3)–C(8A)	59.78(6)	B(6)–B(11)–C(9A)	58.85(6)	B(21)–B(26)–B(25)	59.34(6)
B(1)–B(3)–B(4)	59.69(6)	B(5)–B(11)–B(6)	59.81(6)	B(25)–B(26)–B(27)	60.62(6)
C(7A)–B(4)–C(8A)	57.00(6)	B(23)–B(21)–B(24)	60.20(6)	C(8B)–C(7B)–B(24)	62.42(6)
B(5)–B(4)–C(7A)	58.40(6)	B(24)–B(21)–B(25)	59.46(7)	B(23)–C(7B)–C(29)	61.74(6)
B(1)–B(4)–B(5)	60.41(7)	B(22)–B(21)–B(23)	59.55(6)	B(23)–C(7B)–B(24)	62.10(6)
B(3)–B(4)–C(8A)	58.98(6)	B(25)–B(21)–B(26)	60.54(7)	B(25)–C(8B)–B(27)	63.37(7)
B(1)–B(4)–B(3)	60.07(6)	B(22)–B(21)–B(26)	60.01(6)	C(7B)–C(8B)–B(24)	60.69(6)
B(4)–B(5)–C(7A)	59.90(6)	B(23)–B(22)–C(29)	59.49(6)	B(24)–C(8B)–B(25)	60.83(6)
B(1)–B(5)–B(4)	59.76(7)	B(21)–B(22)–B(23)	60.06(6)	C(8B)–B(27)–B(25)	58.43(6)
B(1)–B(5)–B(6)	60.05(7)	B(21)–B(22)–B(26)	60.25(6)	B(25)–B(27)–B(26)	59.79(6)
C(7A)–B(5)–B(11)	59.86(6)	B(28)–B(22)–C(29)	59.01(6)	B(26)–B(27)–B(28)	59.24(6)
B(6)–B(5)–B(11)	60.15(6)	B(26)–B(22)–B(28)	59.97(6)	B(22)–B(28)–C(29)	58.02(6)
B(2)–B(6)–C(9A)	59.73(6)	C(7B)–B(23)–C(29)	56.49(5)	B(22)–B(28)–B(26)	59.46(6)
B(1)–B(6)–B(2)	59.72(6)	B(22)–B(23)–C(29)	58.93(6)	B(26)–B(28)–B(27)	59.18(6)
B(1)–B(6)–B(5)	59.94(7)	B(21)–B(23)–B(22)	60.39(6)	C(7B)–C(29)–B(23)	61.77(6)
C(9A)–B(6)–B(11)	58.86(5)	C(7B)–B(23)–B(24)	58.85(6)	B(22)–C(29)–B(23)	61.58(6)
B(5)–B(6)–B(11)	60.04(6)	B(21)–B(23)–B(24)	60.03(6)	B(22)–C(29)–B(28)	62.97(6)

Frequencies in the vibrational spectrum of complex **1** can be assigned to its components — cationic $[H(Phen)_2]^+$ and anionic $[NiCb_2]^-$ — only roughly due to the band overlap. The frequency assignment was based on the results of references [1, 13, 14]. The band of stretching vibrations $\nu(NH^+)$ does not manifest in the IR spectrum. Stretching vibrations ν(CH), here including a superposition of carborane and phenantroline CH bonds, are observed as a weak broad band with the maximum at 3069 cm^{-1}.

IR spectrum of 1, $\nu(cm^{-1})$. Major bands of the anion $[NiCb_2]^-$: ν(BH) — 2615 m, 2592 m, 2563 s, 2543:2532:2527 vs, 2502 s; δ(CH) — 1222 m*, 1157 w; δ(BH) — 1080 m*, 1027 w/m; δ(BH), ν(BB, BC) — 978 m, 925 w, 905 w, 737 m*, 463 w.

Major bands of the cation $[H(Phen)_2]^+$: $\delta(NH^+)$ — 1373 w; ν(CC, CN) — 1618 w, 1596 w, 1594 w/m, 1512 w, 1498 w, 1470 w; δ(CH), ν(CC, CN) — 1422 m, 1345 w, 1252 w, 1157 w, 847 vs, 770 w/m, 624 w.

Fig. 5 shows the Raman spectrum of the complex. Two intensive narrow polarized lines with the maxima at 178 cm^{-1} and 222 cm^{-1} are related to the characteristic fully symmetric stretching vibration of the linear tri-atomic system Cb–Ni–Cb [1], in which the Cb ligand behaves as a pseudoatom.

---

*Overlap of cation and anion bands, s means strong, m — medium, w — weak, v — very.

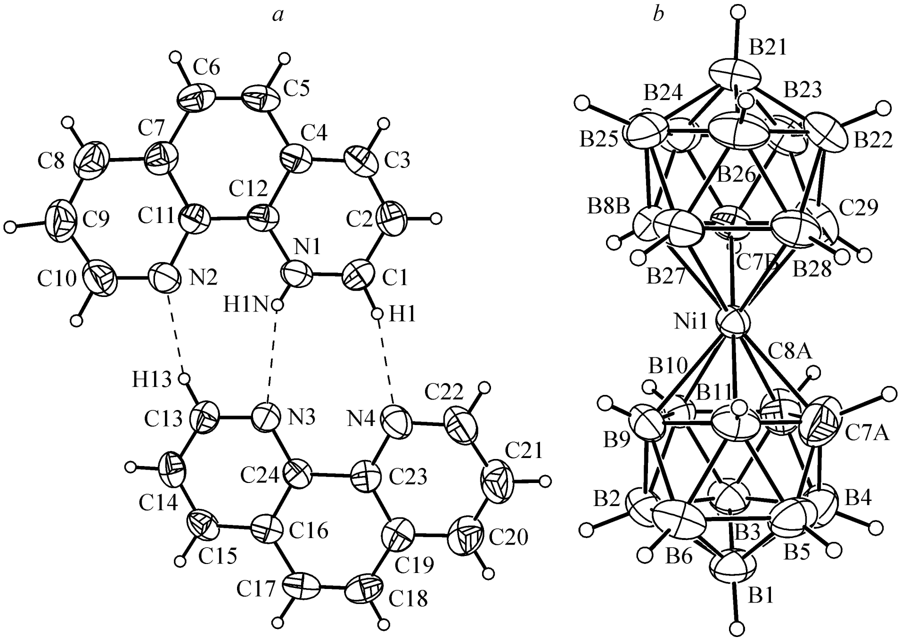

Fig. 1. Structure of the cation $[H(Phen)_2]^+$ (*a*) and the anion $[Ni(B_9C_2H_{11})_2]^-$ (*b*) in the structure of **1**, including atomic labeling. Hydrogen bonds are denoted with dashed lines.

The effective magnetic moment μ_{eff} of Ni(III) in the anion was measured by the Faraday's method at room temperature with correction for a diamagnetic contribution of Cb aromatic cluster ligands.

RESULTS AND DISCUSSION

X-ray structural study of compound **1** reveales that the crystals are built from cations $[H(Phen)_2]^+$ and anions $[NiCb_2]^-$. All atoms of the structure are in general positions. The geometry of the ions together with atomic labeling is shown in Fig. 1.

The cation $H(Phen)_2^+$ comprises a phenantrolinium ion $HPhen^+$ and a phenantroline molecule Phen, as illustrated in Fig. 1*a*, the acidic proton H(1N) is bound to the nitrogen atom N(1). The hydrogen atom is discernable in the differential Fourier map and is localized at the distance N(1)–H(1N) 0.763(8) Å, virtually equal to N–H bond lengths 0.76 Å and 0.74 Å observed in the structures of this cation with single charged anions di-halogeno-(diethyldithiocarbamato)tellurate(II) $[H(Phen)_2][Te(S_2CNEt_2)I_2]$ (**2**) and $[H(Phen)_2][Te(S_2CNEt_2)Br_2]$ (**3**), respectively [15], but shorter than in the structure with inorganic anion ClO_4^- (**4**), in which N–H bonds are 0.96(3) Å and 1.05(3) Å for two crystallographically different cations [16].

The cation itself is non-planar although both of its constituents are practically planar. In **1,** the dihedral angle between their planes is 25.3°. For complexes **2** and **3,** it is equal to 55.9° and 57.8°, for the complex **4,** containing two independent cations, 38.9° and 42.6°. Two fragments of the cation are joined by three hydrogen bonding interactions. The major one is between the acidic proton and atom N(3) of the Phen molecule. The distance N(1)···N(3) equal to 3.103(1) Å is longer than analogous distances observed in complexes **2**-**4**: 2.845 (**2**) Å, 2.842 (**3**) Å, 3.00(3) Å, and 3.01(3) Å (**4**). A decrease in the angle between two aromatic angles in **1** is accompanied by the increased repulsion, and two nitrogen atoms make a weaker and longer hydrogen bond. This is in accord with the correlation found in [17], stating that the angle between two Phen molecules hydrogen-bonded is related to the distance between two nitrogen atoms. In compound **1,** the distance H(1N)···N(3) is 2.426(9) Å; the angle N(1)–H(1N)···N(3) equals 149(1)°. Similar angles in compounds **2**-**4** are: 159° (**2**), 162° (**3**), 166(1)°, and 158(1)° in (**4**). In **1,** two fragments of the cation exhibit two additional interactions. Each of the *ortho* hydrogen atoms H(C), neighboring to nitrogen atoms involved in the bond N(1)–H(1N)···N(3), make a close contact to the free nitrogen atom of the opposite phenantroline system, thus giving the hydrogen bonds [C(1)···N(4) 3.182(1) Å, H(1)···N(4) 2.356(8) Å, C(1)–H(1)···N(4) 149°; C(13)···N(2) 3.285(1) Å, H(13)···N(2) 2.482(8) Å, C(13)–H(13)···N(2) 145°] (Fig. 1*a*). The distances between carbon and nitrogen atoms in the compounds under comparison are: 3.348 Å and 3.399 Å (**2**); 3.299 Å and 3.380 Å (**3**); 3.07(2) Å, 3.07(3) Å and 3.13(3) Å, 3.19(2) Å for two cations in **4**. Corresponding distances H···N are: 2.71 Å and 2.59 (**2**) Å; 2.64 Å and 2.72 Å (**3**); 2.49 Å, 2.52 Å and 2.54 Å, 2.58 Å in (**4**).

In **1,** the geometrical characteristics of Phen fragments generally match each other and the literature data, including the individual molecule of 1,10-Phen [18]. Bond lengths C–N and C–C vary within 1.319(1)-1.366(1) Å and 1.340(1)-1.452(1) Å, mean values 1.341(1) Å and 1.396(1) Å, respectively. Bonds C(5)–C(6) 1.340(1) Å and C(17)–C(18) 1.341(1) Å are shortest and approach the value for the double bond C=C. An observable difference (0.0189 Å) between the longest chemically equivalent bonds C(11)–C(12) and C(23)–C(24) in two fragments of the cation in **1** was also noted for crystallographically distinct molecules of individual Phen [18].

Although both cation fragments are practically planar, the dihedral angle between the planes of pyridine and pyridinium rings in HPhen is 2.1°, while this angle between the planes of pyridine fragments of Phen equals 2.0°. The internal angle C(1)–N(1)–C(12) 122.58(7)° in the cation at the protonated nitrogen atom is substantially larger that at non-protonated ones falling within the range from 117.05(7)° at N(4) to 117.52(7)° at N(3) and the values found for 1,10-Phen [18]. This is in accord with the data on other structures comprising cations H(Phen)$_2^+$ and (HPhen)$^+$ deposited in the Cambridge structural database. The cations make stacks along the *b* axis — the shortest translation of the unit cell.

The anion NiCb$_2^-$ is built from two icosahedra sharing a common vertex occupied with Ni(III) ion (Fig. 1*b*). Two planes {C_2B_3} coordinate the Ni atom in the η^5 mode providing the pentagonal antiprismatic environment of the central atom. In one of {C_2B_3} planes, two carbon atoms are statistically disordered over four boron positions, i.e., each position is simultaneously occupied with carbon and boron atoms with the occupation factor of 0.5. In the other {C_2B_3} plane, one of carbon atoms fully occupies its site, while the second one manifests a statistical disorder over two positions with the occupation factor 0.5. Rms planes defined by two pentagonal faces {C_2B_3} are almost parallel with the tilt of 3.1°. Ni atom is separated from them by 1.558 Å and 1.561 Å, practically the same as in the structure of [Me_4N][$NiCb_2$] (**5**) (1.556 Å) [19], but essentially farther than in the structure of [$MnPhen_3$][$NiCb_2$]$_2$ (**6**) for both crystallographically independent anions (1.460 Å, 1.457 Å and 1.474 Å, 1.477 Å respectively) [10]. This indicates some evolution of the electronic structure of the cluster system [$NiCb_2$] when varying the cation type, although XPS data reported in [1] do not support this point.

Five atoms of {C_2B_3} in each face are not exactly coplanar: the faces are bent at the lines C(7A)···B(9) and C(7B)···B(28), and have an envelope conformation with dihedral angles 5.6° and 2.4°, respectively. Lower pentagonal belts B(2)–B(3)–B(4)–B(5)–B(6) and B(12)–B(13)–B(14)–B(15)–B(16) are also bent at the lines B(2)···B(4), B(22)···B(25); for them the envelope conformation is characterized by smaller values of the angles: 3.3° and 1.6°, respectively. The largest deviations from the {C_2B_3} rms planes are: 0.027 Å for C(7A), 0.037 Å B(9), 0.039 Å B(11), 0.016 Å for C(7B), 0.017 Å C(29). Dihedral angles between the pentagonal belts in the ligands *nido*-[7,8-$B_9C_2H_{11}$]$^{2-}$ are 0.4° and 1.4° for the fragments comprising apical atoms B(1) and B(21), respectively. It is worth noting that three bonds Ni–B are shorter than the bond Ni–C [Ni(1)–B(11) = 2.097(1) Å, Ni(1)–B(27) = 2.120(1) Å, Ni(1)–B(28) = 2.125(1) Å, Ni(1)–C(29) = 2.166(1) Å], though the covalent radius of boron atom B(0.88 Å) exceeds that of carbon atom C(0.77 Å). As a result, distances from the Ni atom to coordinating atoms of the carborane ligands fall within 2.097(1)-2.167(1) Å, the distances from the disordered atoms B(C) being intermediate between boundary values for the bonds Ni–B and Ni–C. A similar phenomenon has been observed already in a series of compounds of this anion with other cations. For example, in the structure of **5** four bonds Ni–B 2.108(6) Å are shortest, while the bonds Ni–C are elongated to 2.146(5) Å, and only two bonds Ni–B 2.160(9) Å are longer than Ni–C bonds. In the structure with the tetrathiofulvalenium cation [$C_6H_4S_4$]$^+$ (refcode YEDVIM, CCDC) two bonds Ni–B (2.108(5) Å

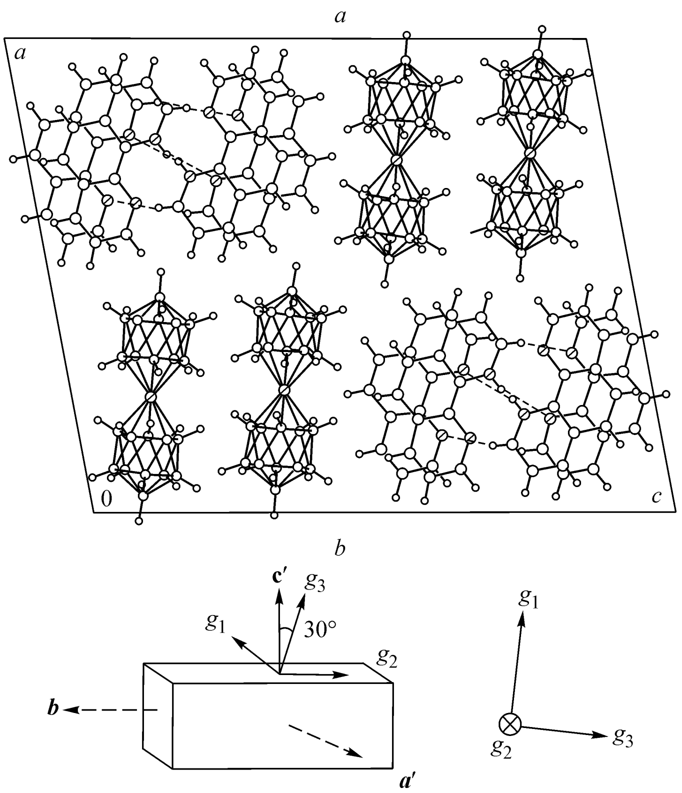

Fig. 2. Projection of the crystal structure of **1** onto the plane (010) (*a*) and orientation of main values of the **g**-tensor to crystal axes and the structure of complex **1** (*b*).

and 2.116(5) Å) are shorter than two bonds Ni–C (2.123(5) Å and 2.151(6) Å), the longest bonds Ni–C and Ni–B being equal (2.151 Å). Hence, all bonds of Ni atom fall within 2.091(4)-2.151(6) Å. This is in accord with the general observation that the metal-boron bonds in electron-rich metallocarboranes are enforced due to metal-carbon bonds.

A shortened contact (C)H···H(B) of 2.28 Å between hydrogen atoms of the cation and anion is found in compound **1**.

The shortest separations between nickel atoms in **1** are 6.813 Å and 6.997 Å. They exceed the similar values (6.357 Å) found before in the crystal structure of **6** [10]. Barycenters of the closest phenantroline and phenantrolinium fragments of the cation are at 7.263 Å and 6.784 Å from the nickel atom, respectively.

Fig. 2*a* depicts a projection of the crystal structure on the plane (010).

EPR spectra of complex 1. The EPR spectrum of a powder sample of complex **1** at 300 K, shown in Fig. 3*a*, is an almost symmetrical single broad line with the half-width $\Delta H_{1/2} \sim 194.6$ G and $g = 2.0374$. When the temperature is lowered to 77 K, the EPR spectrum lines of the complex are narrowed and anisotropy of the *g*-factor is resolved (Fig. 3*b*). The experimental EPR spectrum of complex **1** at 77 K is well-reproduced with *g*-factor values: $g_1 = 2.0803$, $g_2 = 2.0229$, and $g_3 = 1.9810$. The average is $g_{\text{av}} = 2.0280$ differing from the value of the *g*-factor of the EPR spectrum at 300 K.

EPR spectra of intentionally grown single crystals were also measured. The crystals have a shape of platelets elongated along the *b* axis of the unit cell (Fig. 2*b*). Let us denote the directions normal to the wide and the narrow faces of the crystal as *a*′ and *c*′, respectively, the direction *a*′ corresponding to the long diagonal (*a*–*c*) of the unit cell (Fig. 2*a*).

The angular dependence of the EPR spectrum of nickel ions examined in the single crystal reveales that in the plane *bc*′ the *g*-factor exhibits minor variations, and the main value of the **g**-tensor, $g_2 = 2.0229$, is directed parallel to the crystal axis *b*. The investigation of the EPR spectrum angular dependence of the nickel complex in the plane *a*′*c*′ (Fig. 4) indicates that the maximum value of the *g*-factor, $g_1 = 2.0803$, corresponds to the direction Cb–Ni–Cb and makes an angle of 30° to the axis *a*′, the **g**-tensor main value $g_3 = 1.9804$ laying in the plane *a*′*c*′ with the angle of 30° to the axis *c*′.

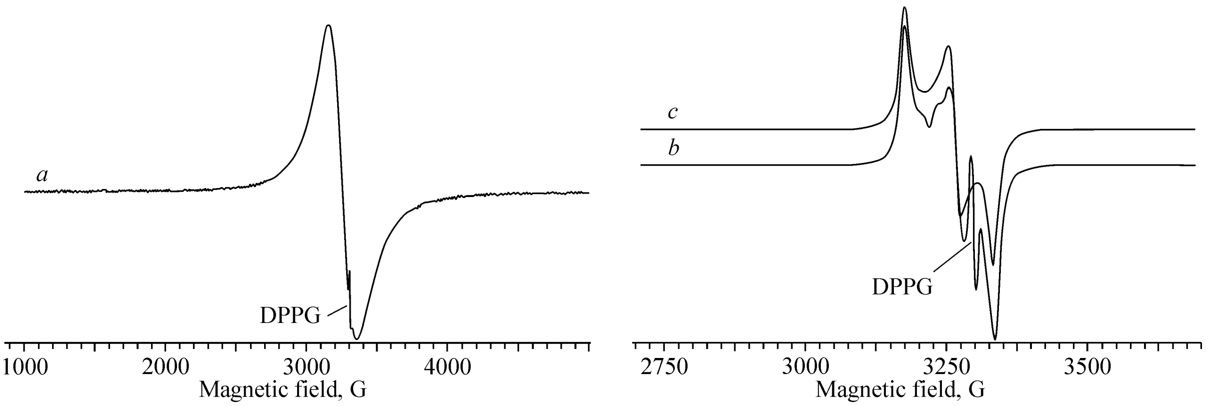

Fig. 3. EPR spectra of powder samples of complex **1**: $T = 300$ K (*a*), 77 K (*b*), simulation for 77 K (*c*).

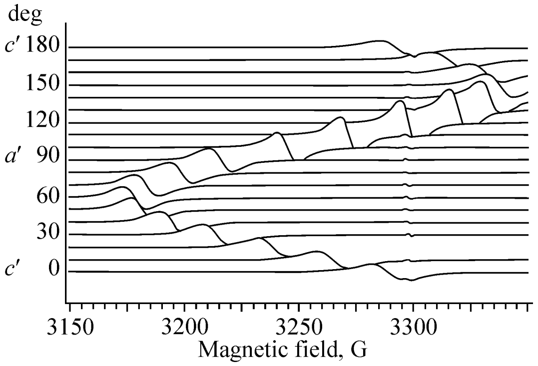

Fig. 4. Angular dependence of the EPR spectrum of nickel ions in the plane ***ac*** of a crystal of **1**. EPR spectra at the angles 60° and 150° correspond to the main value directions g_1 and g_3 of the **g**-tensor.

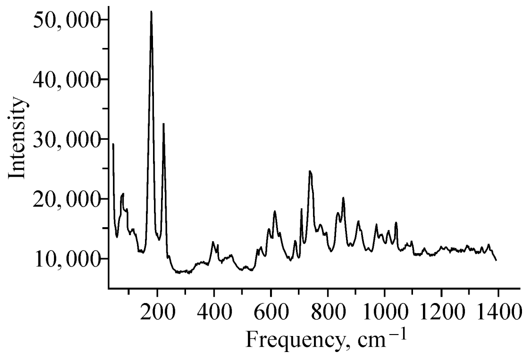

Fig. 5. Raman spectrum of the complex $[H(Phen)_2]$ $[Ni(B_9C_2H_{11})_2]$.

g-Factor values for complex **1** are different from similar values for the previously studied complexes with univalent cations $[Me_4N][NiCb_2]$ **5** ($g_1 = 2.1080$, $g_2 = 2.0323$, $g_3 = 1.959$), $Cs[NiCb_2]$ **7** ($g_1 = 2.096$, $g_2 = 2.032$, and $g_3 = 1.980$), $[TSeT][NiCb_2]$ **8** (TSeT = tetraselenotetracene $[(C_{18}H_8Se_4)_2]^+$, $g_1 = 2.0688$, $g_2 = 2.0332$, $g_3 = 1.9707$) and $[TTT][NiCb_2]$ **9** (TTT tetrathiotetracene $[(C_{18}H_8S_4)_2]^+$, $g_1 = 2.0895$, $g_2 = 2.0217$, $g_3 = 1.9697$), which have the same structural fragment around nickel ion and differing by cations [10, 20]. According to calculations reported in [21, 22], for the ground state $d_{x^2-y^2}$ for both complex **1** under study and **5**, **7-9** studied before, one of the main values of the **g**-tensor larger than two ($g_1 > 2$) corresponds to the direction Cb–Ni–Cb.

The observed distinctions in the parameters of nickel ion spectra originate from distortions introduced by the cation, and are explained by the fact that for $[H(Phen)_2]^+$, Cs^+, $(TSeT)^+$, $(TTT)^+$, and $[Me_4N]^+$ cations the positive charge delocalizes over the cation fragment differently and actually produces different perturbations of the crystal field around nickel ion. This causes the electron density re-distribution and affects the values of the *g*-factor. As reported in [23], for frozen solutions of complex **5** the *g*-factor is isotropic within the plane perpendicular to the direction Cb–Ni–Cb, and the largest *g*-factor corresponds to the Cb–Ni–Cb direction. In crystalline **5,** the direction Cb–Ni–Cb is also characterized by the maximal value of the *g*-factor, and in the plane perpendicular to Cb–Ni–Cb there is a special direction corresponding to the main value g_2 of the **g**-tensor, which is related to the shortest contact with the cation [10]. The quantities given evidence that in all complexes in question g_3 is less than two and is virtually insensitive to the variation of the complex, while g_2 strongly depends on the cation nature, and its evolution is most likely to be governed by a distortion the crystal field around nickel ion caused by the cation.

The observed electron spin $S = 1/2$ of Ni(III) ion in the anions of complexes **1**, **5-8** corresponds to the configuration $3d^7$ with the orbital triplet as the ground state. According to EPR theory for sandwich structures developed by Robertson and McConnell in [21], six d-electrons of nickel ion occupy three levels of the orbital triplet yielding a total electron spin $S = 0$. The seventh electron giving the electron spin $S = 1/2$ resides either on d_{yz}, d_{xz} or $d_{x^2-y^2}$ antibonding orbitals. Calculations afford $g_z < 2$ and g_x, $g_y > 2$ for planar complexes with the d_{z^2} ground state. The experimental g-factor values for the complexes with cations $[H(Phen)_2]^+$, $[Me_4N]^+$, $[TTT]^+$, $[TSeT]^+$ and Cs^+ correspond to the $d_{x^2-y^2}$ ground state of nickel ion and agree with the above theoretical calculations [21, 22] with $g_z > 2$ and g_x, $g_y \sim 2$.

As in the studied compound, the shortest separations between nickel ions are 6.813 Å and 6.997 Å, dipole-dipole interactions between nickel ions will be about several dozens of Gauss. On the whole, this should result only in EPR line broadening. The observed temperature evolutions in powder EPR spectra of complexes containing different functional groups in the cation fragment are determined by a distortion of the nickel ion environment due to cation lability causing the re-distribution of the unpaired electron density, and, hence, of the average g-factor.

The μ_{ef} value for the $3d^7$ configuration of Ni in compound **1** is equal to 1.74 BM.

CONCLUSIONS

The X-ray diffraction structural study revealed that bis-[η^5-π-1,2-(3)-dicarbollyl]nickelate(III) $(NiCb_2)^-$ forms with $[H(Phen)_2]^+$ a compound of $[H(Phen)_2]^+(NiCb_2)^-$ composition. There were obtained and analyzed the geometrical characteristics of ionic fragments comprising the structure, including three hydrogen bonds $X–H\cdots N$, $X = N, C$ stabilizing the cation. An enhancement of a number of nickel-boron bonds due to nickel-carbon bonds was found.

EPR studies showed that nickel ion in the investigated complex has the electron state $3d^7$ with the electron spin $S = 1/2$. The observed values of g-factors correspond to the $d_{x^2-y^2}$ state of nickel ion in the sandwich structure. The angular dependence of single crystal EPR spectra was used to assign the directions of the main values of the **g**-tensor. It was found that the direction $g_1 > 2$ corresponds to the line Cb–Ni–Cb, while the direction and g_2 value are determined by a distortion introduced by the cation.

The authors are grateful to Dr. A. V. Virovets for his assistance in the X-ray diffraction study, Prof. V. N. Ikorskii for the magnetic susceptibility measurement, and Prof. B. A. Kolesov for the recording of Raman spectra.

REFERENCES

1. V. V. Volkov, E. A. Il'inchik, B. A. Kolesov, et al., *Zh. Strukt. Khim.*, **37**, No. 6, 1060-1071 (1996).
2. V. V. Volkov, T. M. Polyanskaya, C. Price, et al., *Khimiya v interesakh ustoichivogo razvitiya*, **8**, Nos. 1/2, 229-236 (2000).
3. T. M. Polyanskaya, V. V. Volkov, and M. K. Drozdova, *Zh. Strukt. Khim.*, **44**, No. 4, 690-700 (2003).
4. V. V. Volkov, V. N. Ikorskii, M. K. Drozdova, et al., *ibid.*, No. 5, 890-896.
5. T. M. Polyanskaya, V. V. Volkov, and M. K. Drozdova, *ibid.*, **46**, No. 4, 730-740 (2005).
6. R. Hoffmann and W. N. Lipscomb, *J. Chem. Phys.*, **36**, No. 12, 3489-3493 (1962).
7. J. Aihara, *J. Am. Chem. Soc.*, **100**, No. 11, 3339-3342 (1978).
8. M. F. Hawthorne, D. C. Young, T. D. Andrews, et al., *ibid.*, **90**, No. 4, 879-896 (1968).
9. E. L. Muetterties (ed.), *Boron Hydride Chemistry*, Academic Press, New York (1975).
10. V. A. Nadolinnyi, T. M. Polyanskaya, V. V. Volkov, et al., *Koordinats. Khim.*, **31**, No. 6, 403-414 (2005).
11. A. Altomare, M. C. Burla, M. Camalli, et al., *J. Appl. Crystallogr.*, **32**, 115-119 (1999).
12. G. M. Sheldrick, *SHELXL-97, Release 97-2*, Univ. Göttingen, Germany (1998).

13. J. S. Strukl and J. L. Walter, *Spectrochim. Acta* (*A*), **27**, No. 2, 209-221 (1971).
14. E. König and K. Madeja, *ibid.*, **23**, No. 1, 45-54 (1967).
15. R. Krishnakumar, G. Aravamudan, M. R. Udupa, et al., *J. Chem. Soc., Dalton Trans.*, No. 11, 2253-2259 (1996).
16. L. Maresca, G. Natile, and F. P. Fanizzi, *J. Am. Chem. Soc.*, **111**, No. 4, 1492/1493 (1989).
17. K. Hensen, F. Gebhardt, and M. Bolte, *Acta Crystallogr.*, **C54**, No. 3, 359-361 (1998).
18. S. Nishigaki, H. Yoshioka, and K. Nakatsu, *ibid.*, **B34**, No. 3, 875-879 (1978).
19. F. V. Hansen, R. G. Hazell, C. Hyatt, et al., *Acta Chem. Scand.*, **27**, No. 4, 1210-1218 (1973).
20. P. A. Chetcuti, W. Hofherr, A. Liegard, et al., *Organometallics*, **14**, No. 2, 666-675 (1995).
21. R. E. Robertson and H. M. McConnell, *J. Phys. Chem.*, **64**, No. 1, 70-77 (1960).
22. Y.-H. Huang, J.-B. Park, M. W. W. Adams, et al., *Inorg. Chem.*, **32**, No. 4, 375/376 (1993).
23. R. J. Wiersema and M. F. Hawthorne, *J. Am. Chem. Soc.*, **96**, No. 3, 761-770 (1974).